

Calculation of core-level electron spectra of ionic liquids

Meeri Lembinen¹, Ergo Nõmmiste¹, Heigo Ers¹, Borja Docampo-Álvarez¹, Jaanus Kruusma¹, Enn Lust¹, and Vladislav Ivanistsev¹

¹Tartu Ulikool

May 5, 2020

Abstract

On the example of forty ion pairs, the study demonstrates how the core-level binding energy values can be calculated and used to plot theoretical spectra at a low computational cost using density functional theory methods. Three approaches for obtaining the binding energy values are based on delta Kohn–Sham (Δ KS) calculations, 1s Kohn–Sham orbital energies, and atomic charges. The Δ KS results show a good agreement between the available experimental X-ray photoelectron data. 1s Kohn–Sham orbital energies and atomic charges also correlate with the Δ KS results.

Calculation of core-level electron spectra of ionic liquids

Meeri Lembinen, 11*Institute of Physics, University of Tartu, Ostwaldi 1, Tartu 50411, Estonia* **Ergo Nõmmiste**, 22*Ergo Nõmmiste deceased 11 April 2019**Institute of Physics, University of Tartu, Ostwaldi 1, Tartu 50411, Estonia* **Heigo Ers**, 33*Institute of Chemistry, University of Tartu, Ravila 14a, Tartu 50411, Estonia* **Borja Docampo-Álvarez**, 44*Institute of Chemistry, University of Tartu, Ravila 14a, Tartu 50411, Estonia* **Grupo de Nanomateriales, Fotónica e Materia Branda, Departamento de Física de Partículas, Universidade de Santiago de Compostela, Campus Vida s/n E-15782, Santiago de Compostela, Spain** **Jaanus Kruusma**, 55*Institute of Chemistry, University of Tartu, Ravila 14a, Tartu 50411, Estonia* **Enn Lust**, 66*Institute of Chemistry, University of Tartu, Ravila 14a, Tartu 50411, Estonia* **and Vladislav B. Ivaništšev** 77*Institute of Chemistry, University of Tartu, Ravila 14a, Tartu 50411, Estonia*

Correspondence to: Vladislav Ivaništšev (E-mail: Vladislav.ivanistsev@ut.ee)

Introduction

X-ray photoelectron spectroscopy (XPS) is a powerful tool for studying the electronic structure of solids, liquids, gases as well as of structures formed at interfaces. It also helps in resolving the atomistic structure by comparing the measured core-level binding energies (BEs) to the reference values.¹ When the appropriate reference values are either not available or not directly applicable, calculations offer a solution for that problem. Among possible methods, density functional theory (DFT)² computations allow analysing electronic and atomistic structures along with predicting BEs for a theoretical XPS spectrum.

Recently, we have applied the XPS method to study the carbon–ionic liquid (IL) interface properties in connection to its application in the supercapacitors.^{3–5} ILs have a variety of

appealing properties,⁶ yet there are not many XPS reference values for that class of compounds. Villar-Garcia *et al.* conducted experimental work on bulk ILs with imidazolium-based cations with varying anions, covering over 20 ILs.⁷ Men *et al.* investigated bulk ILs based on pyrrolidinium cation and various anions.⁸ Foelske-Schmitz *et al.* studied EMImBF₄, EMImB(CN)₄, and EMImTFSI ILs at the carbon electrode.⁹ Kruusma *et al.* also focused on EMImBF₄ and EMImB(CN)₄ characterisation near electrochemically charged carbon electrode.^{3–5}

Although the DFT methods are well suited for ILs structure and property calculations,^{10,11} computational works on XPS of ILs are sparse. It is surprising as the calculation of the X-ray photoelectron core-level spectra is one of the examples where an ion pair is sufficient for modelling the bulk IL.¹² Generally, the solvate shell causes changes in the electronic and atomistic structures affecting the infrared, ultraviolet and other spectra. The core-level electron spectrum is influenced by the solvation shell to a lesser degree. As the core-levels are determined mostly by the chemical bonding within a molecular entity, hypothetically the BEs should correlate with the atomic charges.¹³ Fogarty *et al.* found such correlation for S(1s) electrons ($R^2 = 0.98$) and N(1s) electrons ($R^2 = 0.94$) between the experimental BEs and the computed atomic charges.^{14,15} Kruusma *et al.* calculated C(1s) electrons' Kohn–Sham orbital energies and used their values for fitting the experimental spectra.³ Similarly, Reinmöller *et al.* used Kohn–Sham orbital energies to calculate the BEs for the XPS spectra.^{16,17}

In this study, we have applied for the first time the delta Kohn–Sham (Δ KS) method for obtaining the BEs of ion pairs. Despite doubts regarding charge transfer in ionic liquids modelled with core-hole,¹⁸ this article demonstrates a good agreement between the available experimental XPS data and the calculated Δ KS BEs. Furthermore, we present and discuss correlations found between the Δ KS BE values, 1s Kohn–Sham orbital energies and atomic charges.

Methods

Binding energy calculation

At the DFT level of theory, the core-level electron BEs can be obtained by applying initial state or final state methods.¹⁹ The final state method includes the core-hole in the electronic structure calculation to get the total energy of the corresponding excited state (E_{exc}). A separate calculation gives the energy of the ground state (E_{gs}). The BE is then obtained as the difference between these two quantities:

$$\text{BE} = E_{\text{exc}} - E_{\text{gs}} \quad (1)$$

On the one hand, since only the energy differences are used, the final state method takes advantage of DFT's high level of accuracy concerning energy differences and neglects inaccuracies arisen by choice of a basis set or a functional used. When applied to small molecules, this approach shows mean absolute errors in the order of 0.2–0.3 eV with respect to experiments.^{20,21} On the other hand, many calculations must be run to obtain BE values for every excited state. Still, the final state method is computationally less expensive than alternatives like the third-order algebraic diagrammatic construction (ADC(3)) method and GW approximation.^{18,22,23} For comparison, the GW method, applied to small molecules, gives mean absolute errors below 0.1 eV.²⁴

The initial state method is computationally even less expensive, as it accounts only for the energy level of the core electron in the ground state. For example, according to Janak's theorem,²⁵ the 1s electron BE can be approximated by a negative Kohn–Sham orbital eigenvalue:

$$\text{BE} [\text{?}] - \epsilon(1s) \quad (2)$$

Although appealing for its simplicity, the initial state method is sensitive to the choice of the DFT functional and considerably overestimates the BEs.²¹

Besides explicit DFT calculations, the BE can be estimated from a purely electrostatic model. Considering a core electron to be localised entirely at its mother-atom, one may assume that its orbital energy is determined by the electrostatic potential near the atomic nucleus. Consequently, the corresponding BE value (via Eq. 2) depends on the charge distribution, at first approximation, given by the local charges of the mother-atom and its neighbouring atoms:¹³

$$\text{BE} [\text{?}] - V(q_i, q_j) = kq_i + l \sum_j [\text{?}]_i V_j + m \quad (3)$$

where the q_i is the atomic charge on the given i -th atom, k is proportionality constant, $l = 14.4 \text{ eV} \cdot \text{\AA} / e$, the sum is an estimate for the electrostatic potential of the other atoms, where $V_j = q_j / R_{ij}$, and m is a constant determined by choice of the reference value. For this work, we obtained the k value of $13.45 \text{ eV}/e$ by linear

fitting the 1s Kohn–Sham eigenvalues of C^+ , C , and C^- vs their charge. The value for m was calculated for each ion pair so that the aliphatic $C(1s)$ electron BE value equals to the reference value of 285.0 eV.

Below we refer to the above-described methods of BE calculation as Δ KS (Eq. 1), $\epsilon(1s)$ (Eq. 2), and $V(q)$ (Eq. 3) methods. In the literature, the delta Kohn–Sham method is also known as delta self-consistent field (Δ SCF);²¹ Janak’s theorem is commonly viewed as an analogue of Koopman’s theorem.²⁶ Only a few codes can run calculations with the core-hole required for the Δ KS method. The $\epsilon(1s)$ method is more accessible than the Δ KS method, yet the basis set used must describe the 1s orbital, which is somehow problematic for the plane wave basis sets. The $V(q)$ method is probably the most universal, yet it depends on the type of atomic charges used in Eq. 3.

The results of the described Δ KS, $\epsilon(1s)$, and $V(q)$ methods can be improved in several ways. In principle, they should converge upon increasing the model size. The smallest IL model is an ion; adding a counter-ion to it creates a solvate shell and introduces ion-ion interactions – from the weak dispersion and hydrogen-bonding to the much stronger ion-ion Coulomb interaction. Taking more than one ion into account affects the results but also increases the cost of the calculations. Similarly, at the computational cost, the absolute BE values can be more accurately calculated by applying an asymptotically correct exchange-correlation potential, for example, via hybrid functionals.²⁷ Knowing all that, we made a pragmatic choice in favour of a simpler model and a common functional to save resources for calculating a more extensive set of ILs.

Computational details

All DFT calculations were performed using the real-space grid-based projector-augmented wave DFT code (GPAW 1.2).^{28–31} In all calculations, we used the projector-augmented wave (PAW) method within the Perdew–Burke–Ernzerhof (PBE) generalised gradient approximation,^{32,33} a grid spacing of 0.16 Å, and the residual minimisation method – direct inversion in iterative subspace (RMM-DIIS).^{34,35} Compared to the most accurate functionals, PBE shows slightly lower performance in respect to the dissociation energy for the chosen set of IL ion pairs.^{36–38} However, PBE is sufficiently fast and accurate for the Δ KS type calculations that give the total energy difference between the ground state and the first core-excited state.^{39,40} To obtain the 1s Kohn–Sham orbital eigenvalues of selected atoms, we generated all-electron setups using gpaw-setup tool with the parameter `-core=""`. All other calculations were run with a default frozen core for GPAW setup 0.9.2.

The gas-phase relaxed structures of ion pairs were taken from Refs 10,37, where they were optimised with B2PLYP double hybrid functional and triple-zeta basis set. Forty different IL ion pairs, all depicted in Figure 1, were formed by combining eight anions ($B(CN)_4^-$, $TFSI^-$, FSI^- , PF_6^- , BF_4^- , Cl^- , Br^- , I^-) with five cations ($EMIm^+$, $BMIIm^+$, $BMPyr^+$, BPy^+ , $TEPA^+$). We introduced 8 Å of vacuum between an ion pair and the side of the calculation box. Convergence problems occurred for several carbon and nitrogen atoms in $BPyTFSI$ and $BPyTFSI$, as well as for few carbon atoms in $BPyB(CN)_4$, $TEPAI$, $TEPABr$, $BMPyrI$, $BMPyrBr$. To tackle this issue, we changed the convergence criterion for energy from 10^{-8} to 10^{-4} and density criterion from default 10^{-4} to 10^{-2} . In the Supplementary information, Table S1 shows how the variation of the named criteria influences the energy values starting from the third decimal point, which can be considered insignificant for the Δ KS type calculations. The Supplementary information also includes all calculated Δ KS BE values.

To automate calculations, we used the NaRIBaS framework – a collection of scripts that allows generating input files for all the required systems by defining all the variables one wishes to combine.⁴¹ To conduct charge localisation analysis of atoms, we used density derived electrostatic and chemical (DDEC6) charges.^{42–44}

Results and discussions

Binding energy and the photoelectron spectra

Figure 2 shows spectra obtained in the experimental XPS measurements in contrast to those plotted using the BE calculated via the Δ KS method. Note that an experimental measurement produces a spectrum which is then interpreted by researchers so that the BE values obtained by the *deconvolution* are manually assigned

to individual atoms. On the contrary, calculations give BE values for individual atoms and the spectrum is obtained by *convolution* of their Gaussian functions with a standard deviation of 0.5 eV.

Furthermore, during experiments, the measured spectrum might shift due to the instability of spectrometer and studied IL as well as due to photoelectron emission. To eliminate the systematic drift, measured BE values are corrected by shifting the spectrum so that the aliphatic C(1s) electron BE value equals to a reference value of 285.0 or 285.3 eV (see Ref 7 and references therein). The choice of the reference is disputable, and it introduces a man-made difference between the shifted experimental and absolute computational values. Also, the reference energy levels in experiment and computation – Fermi and vacuum energy, respectively – do not necessarily match each other. Table 1 shows that the calculated Δ KS BEs for the aliphatic carbon are higher than the reference value of 285 eV by 4–5 eV. Most of that difference is an artefact, while a part is due to the inaccuracy of the method. For example, in the case of $\epsilon(1s)$ method, the difference can be dumped by correcting the result with the Perdew–Zunger self-interaction error correction (see Table 2).^{45,46} For a fair comparison, below we denote as *relative* BEs all values shifted so that the aliphatic C(1s) electron BE value equals to the reference value. When both experimental and predicted spectra are shifted in the same way, as in Figure 2, a reasonably good agreement between the experimental data and Δ KS results becomes visible. Bearing in mind that an ion pair is the simplest model of a bulk IL, we leave the explanation of minor deviations to future work on modelling of bulk ILs.

Figure 3 depicts isosurfaces of the charge density difference between the positively charged excited state and the neutral ground state of EMImBF₄ – the positive value corresponds to a loss of electron density. Recently Golze *et al.* hypothesised that the negative charge at an anion could displace to neutralise the core-hole at a cation atom in the excited ion pair.¹⁸ As can be seen in Figure 3, there is no notable partial charge transfer between the BF₄[−] anion and the EMIm⁺ cation; a small redistribution of the electron density happens only in the vicinity of the carbon atom with a full core-hole.

Figure 4 compares experimental and theoretical spectra for EMImBF₄, which is one of the most studied ILs by the XPS method. All spectra shown have a very similar shape, yet, as can be anticipated, there is a difference in the sequence of the peaks associated with specific carbon atoms. All BE values are given in Table 1 as well as marked in Figure 4 with rounded numbers corresponding to *inter* atoms C1, C2, and C3 of the imidazolium ring, *chain* atoms C4 and C5 connected to the nitrogen atoms, an *aliphatic* C6 (as defined in Figure 3). The IUPAC atom numbering is also given in Table 1 to simplify the comparison with the literature.

In comparison to the previously reported BE sequences data for EMImBF₄, the Δ KS method swaps the order of C2/C3 and C4/C5 peaks (see Table 2 and Figure 4). As stated above, the assignment of peaks to certain atoms is somehow arbitrary. In case of imidazolium-based ILs, the widely accepted order originates from work 47, where no clear reasoning is given. Later, Kruusma *et al.* and Reinmöller *et al.* used calculated C(1s) Kohn–Sham orbital energies for reconstructing the experimental spectra.^{3,16} Accordingly, their results are in agreement with our calculated $\epsilon(1s)$ BEs position in the spectra. However, BEs obtained via Eq. 2 are only approximate, as the negative eigenvalues of orbitals below ϵ_{HOMO} do not precisely correspond to the vertical ionisation potential.⁴⁸ Moreover, the $\epsilon(1s)$ method neglects the electron density relaxation effects in response to the core-hole creation illustrated in Figure 3. It was also previously shown that Δ KS method provides much more accurate predictions than Janak’s or Koompan’s theorem-based calculations.²¹ Finally, the most recent difference spectroscopy study resolved the order of peaks in favour of the Δ KS method.⁴⁹ We conclude that the Δ KS method does give more reliable results than the $\epsilon(1s)$ method.

Figure 5 demonstrates a correlation between the relative Δ KS BEs and the relative $\epsilon(1s)$ BEs for forty ion pairs. Despite a good correlation with $R^2 = 0.93$, the standard deviation of 0.32 eV allows swapping the order of peaks in spectra, as can be seen in case of EMImBF₄. When the order of BEs is essential, the Δ KS method or even better, the GW method should be used.^{21,50,51} Nonetheless, because the $\epsilon(1s)$ method is computationally cheaper and more accessible, it can be used for predicting XPS spectra of larger systems as well as in longer simulations, especially with periodic boundary conditions. GW or Δ KS methods are currently impractical for large systems. The most recent implementation of the GW method for massively

parallel execution applies to systems up to 100 atoms.^{18,52} The Δ KS method requires additional calculations for each BE value, making it substantially more resource-demanding than the $\epsilon(1s)$ method. Therefore, the use of the $\epsilon(1s)$ method is justified for large systems, *e.g.* complex interface models calculated with DFT (with or without periodic boundary conditions) or simulated with DFT-based molecular dynamics, discussed in Refs^{53–57}. $\epsilon(1s)$ method might also be useful when the changes in the XPS spectra upon variation of the chemical composition are a focus of a study, for example, in studies of interfacial reactions.⁵⁸

Binding energy correlation with orbital energy and atomic charges

Recently it was proposed that the BEs obtained from fitting of the experimental XPS spectra for ILs correlate with the calculated atomic charges.^{14,15} Figure 6 demonstrates a modest correlation between the BE approximated by the first and third terms of Eq. 3 ($BE = V(q_i)$) and the calculated relative Δ KS BE values. The relation improves significantly by considering the effect of the electrostatic potential of neighbouring atoms given by the second term in Eq. 3 ($BE [?] V(q_i, q_j)$). Consideration of the neighbour atoms increases the coefficient of determination (R^2) for individual ion pairs (from 0.04–0.65 to 0.35–0.97) as well as for the whole set of forty ion pairs (from 0.28 to 0.83). Nevertheless, the deviations allow the difference in the order of BEs calculated via Δ KS and $V(q)$ methods.

It should be noted that the $V(q)$ method has an excessive cost in comparison to the $\epsilon(1s)$ method – it calls for more resources to perform the charge analysis. For example, for the studied ion pairs, the DDEC6 analysis is almost as demanding as a single point DFT calculation. On the bright side, charge analysis does not require all-electron basis sets, allowing the application of pseudopotentials and effective core potentials to recoup the cost of any post-analysis.

Conclusions

In this work, we have validated the applicability of density functional theory (DFT) methods to the prediction of the X-ray photoelectron spectra (XPS) of ionic liquids. On the example of data for forty ion pairs, we demonstrated how the core-level electron binding energy (BE) could be calculated and used to plot theoretical spectra at a low computational cost. The delta Kohn–Sham (Δ KS) method provides the most reliable results in comparison to the experimental spectra. Negative 1s Kohn–Sham orbital energies show a strong correlation with the calculated Δ KS BE values. However, the sequence of orbital energies differs from the Δ KS BEs data. The correlation of the calculated atomic charges with the Δ KS BE values is notably weaker. Nonetheless, that correlation can be improved by accounting for the electrostatic potential due to the surrounding atoms in the ion pair. Thus, the XPS spectra can be predicted based on the DFT calculations using three different approaches. The choice between them implies a compromise between the computational cost and accuracy. Besides being more accurate, the Δ KS method is also more resource-demanding and less accessible than the other two methods. The use of 1s Kohn–Sham orbital energies and atomic charges are justified when qualitative aspects of X-ray photoelectron spectra are of higher interest than the absolute binding energy values or when the available computational power is limited.

Acknowledgements

We dedicate this work in memoriam of Prof. Ergo Nõmmiste.

Funding Information

The European Union supported the work through the European Regional Development Fund (TK141, Centre of Excellence, 2014-2020.4.01.15-0011 and 1.01.2016-1.03.2023), Institutional Research Grants IUT20-13 and IUT2-25, and Estonian Personal Research Project PUT1107. Funding from the European Union (COST Actions CM1206 and MP1303) is also acknowledged.

Research Resources

Results were obtained in part using the High-Performance Computing Centre of the University of Tartu.

Keywords: ionic liquid, X-ray photoelectron spectra, core-level binding energy, delta Kohn–Sham, Green function

Additional Supporting Information may be found in the online version of this article.

References and Notes

1. S. Hüfner, *Photoelectron Spectroscopy - Principles and Applications*, Springer Berlin Heidelberg, **2013**.
2. W. Kohn, A. D. Becke and R. G. Parr, *J. Phys. Chem.*, **1996**, 100, 12974–12980.
3. J. Kruusma, A. Tõnisoo, R. Pärna, E. Nõmmiste, I. Kuusik, M. Vahtrus, I. Tallo, T. Romann and E. Lust, *J. Electrochem. Soc.*, **2017**, 164, A3393–A3402.
4. J. Kruusma, A. Tõnisoo, R. Pärna, E. Nõmmiste, I. Tallo, T. Romann and E. Lust, *Electrochimica Acta*, **2016**, 206, 419–426.
5. A. Tõnisoo, J. Kruusma, R. Pärna, A. Kikas, M. Hirsimäki, E. Nõmmiste and E. Lust, *J. Electrochem. Soc.*, **2013**, 160, A1084–A1093.
6. P. Wasserscheid and T. Welton, *Ionic Liquids in Synthesis*, John Wiley & Sons, **2008**.
7. I. J. Villar-Garcia, E. F. Smith, A. W. Taylor, F. Qiu, K. R. J. Lovelock, R. G. Jones and P. Licence, *Phys. Chem. Chem. Phys.*, **2011**, 13, 2797–2808.
8. S. Men, K. R. J. Lovelock and P. Licence, *Phys. Chem. Chem. Phys.*, **2011**, 13, 15244–15255.
9. A. Foelske-Schmitz, D. Weingarth and R. Kötz, *Surf. Sci.*, **2011**, 605, 1979–1985.
10. K. Karu, A. Ruzanov, H. Ers, V. Ivaništšev, I. Lage-Estebanez and J. M. García de la Vega, *Computation*, **2016**, 4, 25.
11. E. I. Izgorodina, Z. L. Seeger, D. L. A. Scarborough and S. Y. S. Tan, *Chem. Rev.*, **2017**, 117, 6696–6754.
12. D. Strasser, F. Goulay, M. S. Kelkar, E. J. Maginn and S. R. Leone, *J. Phys. Chem. A*, **2007**, 111, 3191–3195.
13. K. Siegbahn, *ESCA applied to free molecules*, North-Holland Pub. Co., **1970**.
14. R. M. Fogarty, R. Rowe, R. P. Matthews, M. T. Clough, C. R. Ashworth, A. Brandt, P. J. Corbett, R. G. Palgrave, E. F. Smith, R. A. Bourne, T. W. Chamberlain, P. B. J. Thompson, P. A. Hunt and K. R. J. Lovelock, *Faraday Discuss.*, **2017**, 206, 183–201.
15. R. M. Fogarty, R. P. Matthews, C. R. Ashworth, A. Brandt-Talbot, R. G. Palgrave, R. A. Bourne, T. Vander Hoogerstraete, P. A. Hunt and K. R. J. Lovelock, *J. Chem. Phys.*, **2018**, 148, 193817.
16. M. Reinmöller, A. Ulbrich, T. Ikari, J. Preiß, O. Höfft, F. Endres, S. Krischok and W. J. D. Beenken, *Phys. Chem. Chem. Phys.*, **2011**, 13, 19526–19533.
17. A. Ulbrich, M. Reinmöller, W. J. D. Beenken and S. Krischok, *J. Mol. Liq.*, **2014**, 192, 77–86.
18. D. Golze, J. Wilhelm, M. J. van Setten and P. Rinke, *J. Chem. Theory Comput.*, **2018**, 14, 4856–4869.
19. J. L. Cabellos, D. J. Mowbray, E. Goiri, A. El-Sayed, L. Floreano, D. G. de Oteyza, C. Rogero, J. E. Ortega and A. Rubio, *J. Phys. Chem. C*, **2012**, 116, 17991–18001.
20. N. P. Bellafont, G. Á. Saiz, F. Viñes and F. Illas, *Theor. Chem. Acc.*, **2016**, 135, 35.
21. F. Viñes, C. Sousa and F. Illas, *Phys. Chem. Chem. Phys.*, **2018**, 20, 8403–8410.
22. L. S. Cederbaum and W. Domcke, in *Advances in Chemical Physics*, John Wiley & Sons, Ltd, **1977**, vol. 36, pp. 205–344.
23. P. H. P. Harbach, M. Wormit and A. Dreuw, *J. Chem. Phys.*, **2014**, 141, 064113.

24. L. Gallandi and T. Körzdörfer, *J. Chem. Theory Comput.* ,**2015** , 11, 5391–5400.
25. J. F. Janak, *Phys. Rev. B* , **1978** , 18, 7165–7168.
26. A. M. Teale, F. D. Proft, P. Geerlings and D. J. Tozer, *Phys. Chem. Chem. Phys.* , **2014** , 16, 14420–14434.
27. Y. Jin and R. J. Bartlett, *J. Chem. Phys.* , **2018** , 149, 064111.
28. S. R. Bahn and K. W. Jacobsen, *Comput. Sci. Eng.* ,**2002** , 4, 56–66.
29. J. J. Mortensen, L. B. Hansen and K. W. Jacobsen, *Phys. Rev. B* , **2005** , 71, 035109.
30. J. Enkovaara, C. Rostgaard, J. J. Mortensen, J. Chen, M. Dulak, L. Ferrighi, J. Gavnholt, C. Glinsvad, V. Haikola, H. A. Hansen, H. H. Kristoffersen, M. Kuisma, A. H. Larsen, L. Lehtovaara, M. Ljungberg, O. Lopez-Acevedo, P. G. Moses, J. Ojanen, T. Olsen, V. Petzold, N. A. Romero, J. Stausholm-Møller, M. Strange, G. A. Tritsarlis, M. Vanin, M. Walter, B. Hammer, H. Häkkinen, G. K. H. Madsen, R. M. Nieminen, J. K. Nørskov, M. Puska, T. T. Rantala, J. Schiøtz, K. S. Thygesen and K. W. Jacobsen, *J. Phys. Condens. Matter* , **2010** , 22, 253202.
31. A. H. Larsen, J. J. Mortensen, J. Blomqvist, I. E. Castelli, R. Christensen, M. Dulak, J. Friis, M. N. Groves, B. Hammer, C. Hargus, E. D. Hermes, P. C. Jennings, P. B. Jensen, J. Kermode, J. R. Kitchin, E. L. Kolsbjerg, J. Kubal, K. Kaasbjerg, S. Lysgaard, J. B. Maronsson, T. Maxson, T. Olsen, L. Pastewka, A. Peterson, C. Rostgaard, J. Schiøtz, O. Schütt, M. Strange, K. S. Thygesen, T. Vegge, L. Vilhelmsen, M. Walter, Z. Zeng and K. W. Jacobsen, *J. Phys. Condens. Matter* ,**2017** , 29, 273002.
32. M. Ernzerhof and J. P. Perdew, *J. Chem. Phys.* , **1998** , 109, 3313–3320.
33. J. P. Perdew, K. Burke and M. Ernzerhof, *Phys. Rev. Lett.* ,**1996** , 77, 3865–3868.
34. D. M. Wood and A. Zunger, *J. Phys. Math. Gen.* , **1985** , 18, 1343–1359.
35. G. Kresse and J. Furthmüller, *Phys. Rev. B* , **1996** , 54, 11169–11186.
36. I. Lage-Estebanez, A. Ruzanov, J. M. G. de la Vega, M. V. Fedorov and V. B. Ivaništšev, *Phys. Chem. Chem. Phys.* , **2016** , 18, 2175–2182.
37. K. Karu, M. Mišin, H. Ers, J. Sun and V. Ivaništšev, *Int. J. Quantum Chem.* , **2018** , 118, e25582.
38. S. Zahn, D. MacFarlane and E. I. Izgorodina, *Phys. Chem. Chem. Phys.* , **2013** , 15, 13664–13675.
39. T. Olsen, J. Gavnholt and J. Schiøtz, *Phys. Rev. B* ,**2009** , 79, 035403.
40. J. Gavnholt, T. Olsen, M. Engelund and J. Schiøtz, *Phys. Rev. B* , **2008** , 78, 075441.
41. E. Roos Nerut, K. Karu, I. V. Voroshylova, K. Kirchner, T. Kirchner, M. V. Fedorov and V. B. Ivaništšev, *Computation* , **2018** , 6, 57.
42. T. A. Manz and D. S. Sholl, *J. Chem. Theory Comput.* ,**2010** , 6, 2455–2468.
43. T. A. Manz and N. G. Limas, *RSC Adv.* , **2016** , 6, 47771–47801.
44. N. G. Limas and T. A. Manz, *RSC Adv.* , **2016** , 6, 45727–45747.
45. J. P. Perdew and A. Zunger, *Phys. Rev. B* , **1981** , 23, 5048–5079.
46. P. Klüpfel, P. M. Dinh, P.-G. Reinhard and E. Suraud, *Phys. Rev. A* , **2013** , 88, 052501.
47. E. F. Smith, F. J. M. Rutten, I. J. Villar-Garcia, D. Briggs and P. Licence, *Langmuir* , **2006** , 22, 9386–9392.
48. U. Salzner and R. Baer, *J. Chem. Phys.* , **2009** , 131, 231101.
49. C. J. Clarke, S. Maxwell-Hogg, E. F. Smith, R. R. Hawker, J. B. Harper and P. Licence, *Phys. Chem. Chem. Phys.* , **2019** , 21, 114–123.

50. D. Golze, M. Dvorak and P. Rinke, *Front. Chem.* ,**2019** , 7.
51. D. Golze, L. Keller and P. Rinke, *arXiv:1911.08428* ,**2020** .
52. J. Wilhelm, D. Golze, L. Talirz, J. Hutter and C. A. Pignedoli, *J. Phys. Chem. Lett.* , **2018** , 9, 306–312.
53. T. P. C. Klaver, M. Luppi, M. H. F. Sluiter, M. C. Kroon and B. J. Thijsse, *J. Phys. Chem. C* , **2011** , 115, 14718–14730.
54. J. Plöger, J. E. Mueller, T. Jacob and J. Anton, *Top. Catal.* ,**2016** , 59, 792–801.
55. A. Ruzanov, M. Lembinen, H. Ers, J. M. García de la Vega, I. Lage-Estebanez, E. Lust and V. B. Ivaništšev, *J. Phys. Chem. C* ,**2018** , 122, 2624–2631.
56. A. Ruzanov, M. Lembinen, P. Jakovits, S. N. Srirama, I. V. Voroshylova, M. N. D. S. Cordeiro, C. M. Pereira, J. Rossmeisl and V. B. Ivaništšev, *Phys. Chem. Chem. Phys.* , **2018** , 20, 10275–10285.
57. E. Paek, A. J. Pak and G. S. Hwang, *J. Chem. Phys.* ,**2015** , 142, 024701–6.
58. J. Kruusma, A. Tõnisoo, R. Pärna, E. Nõmmiste and E. Lust, *Nanomaterials* , **2019** , 9, 304.
59. T. Hammer, M. Reichelt and H. Morgner, *Phys. Chem. Chem. Phys.* , **2010** , 12, 11070–11080.

Table 2. C(1s) BEs (eV) for EMImBF₄. Values from the literature are given in italics.

Fig. 3 atom nr IUPAC atom

EMImBF₄

EMImBF₄ [1s]

EMImBF₄ [SIC]

EMImBF₄ [d]

EMImBF₄ [e]

[1s] 1s calculation, [SIC] 1s calculation with Perdew–Zunger self-interaction error correction, [d] Taken from Ref 7 (Garcia-V

Table 2. C(1s) BEs (eV) for EMImBF₄. Values from the literature are given in italics.

Fig. 3 atom nr IUPAC atom

EMImBF₄

EMImBF₄ [1s]

EMImBF₄ [SIC]

EMImBF₄ [d]

EMImBF₄ [e]

[1s] 1s calculation, [SIC] 1s calculation with Perdew–Zunger self-interaction error correction, [d] Taken from Ref 7 (Garcia-V

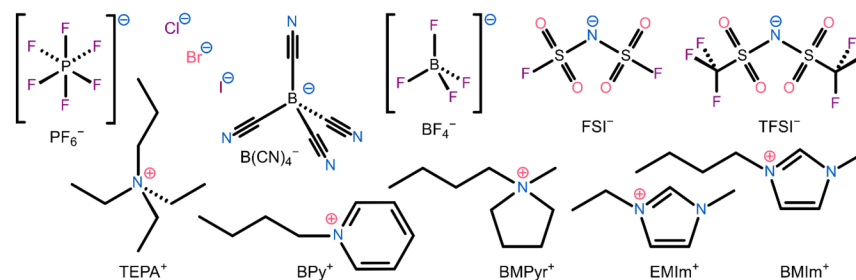


Figure 1. Eight anions and five cations were combined to make up the forty ionic pairs.

Starting from the top left: hexafluorophosphate, chloride, bromide, iodide, tetracyanoborate, tetrafluoroborate, bis(fluorosulfonyl)imide, bis(trifluoromethylsulfonyl)imide. Bottom row represents the cations: triethylpropyl-ammonium, 1-butyl-pyridinium, 1-butyl-1-methylpyrrolidinium, 1-butyl-3-methylimidazolium, 1-ethyl-3-methylimidazolium.

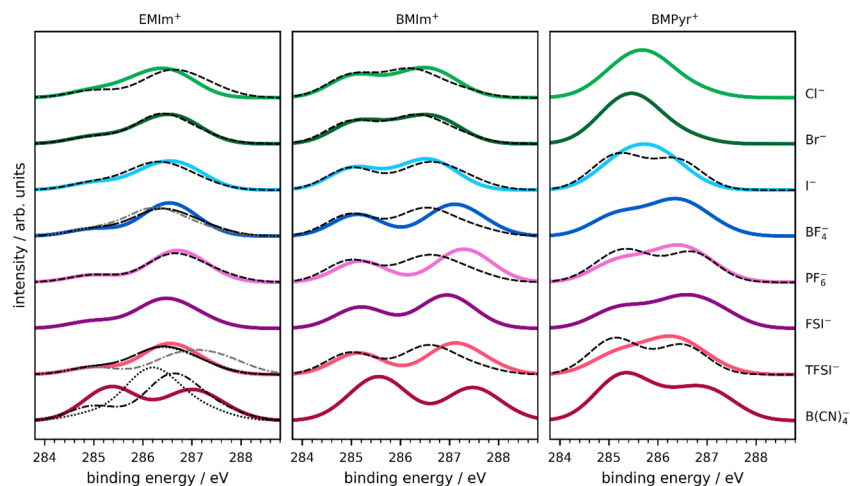


Figure 2. C(1s) XPS spectra for 24 combinations of EMIm⁺, BMIm⁺, and BMPyr⁺ cations with eight anions. The data for continuous lines were calculated in this work. The data for the dotted line is taken from Ref 3, long-dash line – from Ref 5, dashed lines – from Ref 7, dash-dotted lines – from Ref 9, dash-dash-dotted lines – from Ref ⁵⁹.

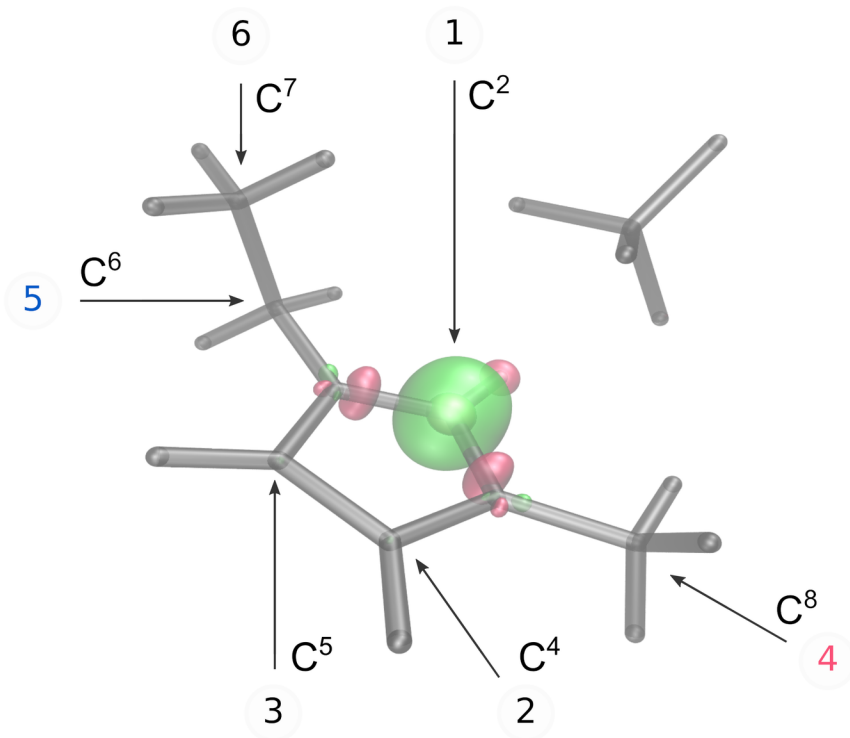


Figure 3. Redistribution of the electron density visualised as the charge density difference between the positively charged excited state and the neutral ground state of EMImBF₄. The green isosurface value equals -0.05 a.u. (an increase of the electronic density). The red isosurface value equals 0.05 a.u. (decrease of the electronic density). Superscripts provide the IUPAC atom numbering. Circled numbers indicate atoms by the data shown in Figure 4 and Tables 1–2.

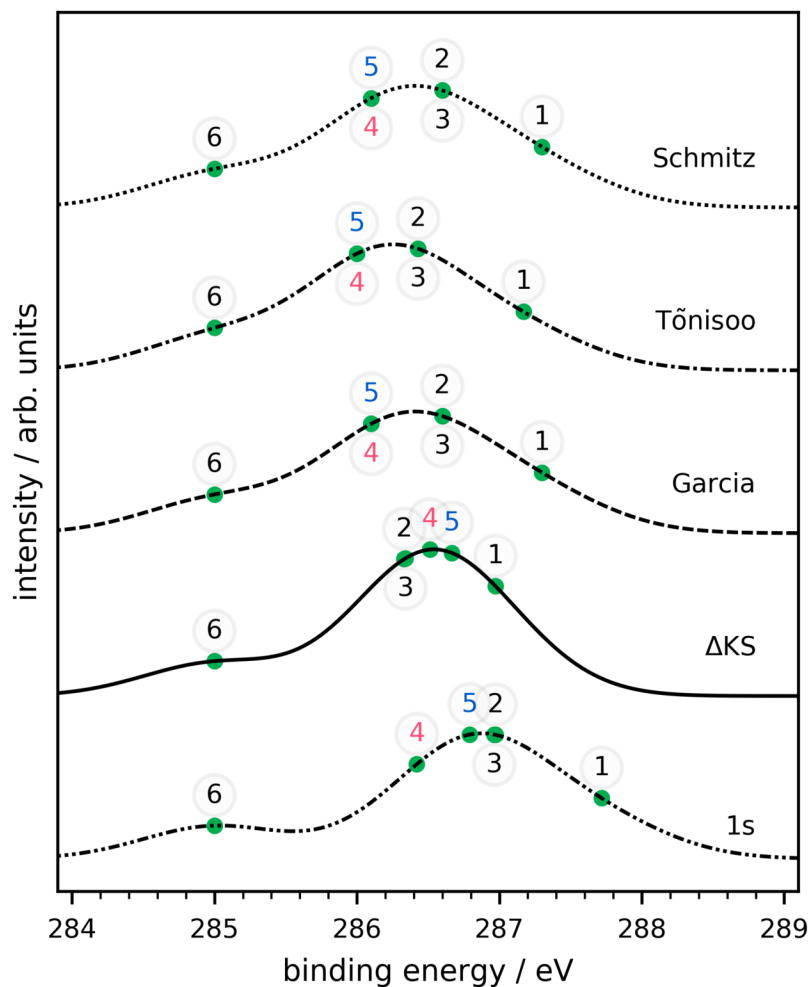


Figure 4. C(1s) XPS spectra of EMImBF₄ obtained using the relative BE values. The data for dot-dashed (1s) and continuous (Δ KS) lines were calculated in this work. The data for the dashed line (Garcia) is taken from Ref 7, dash-dotted line (Tõnisoo) – from Ref 5, dotted line (Schmitz) – from Ref 9. Absolute BE values for the labelled data points are given in Table 2.

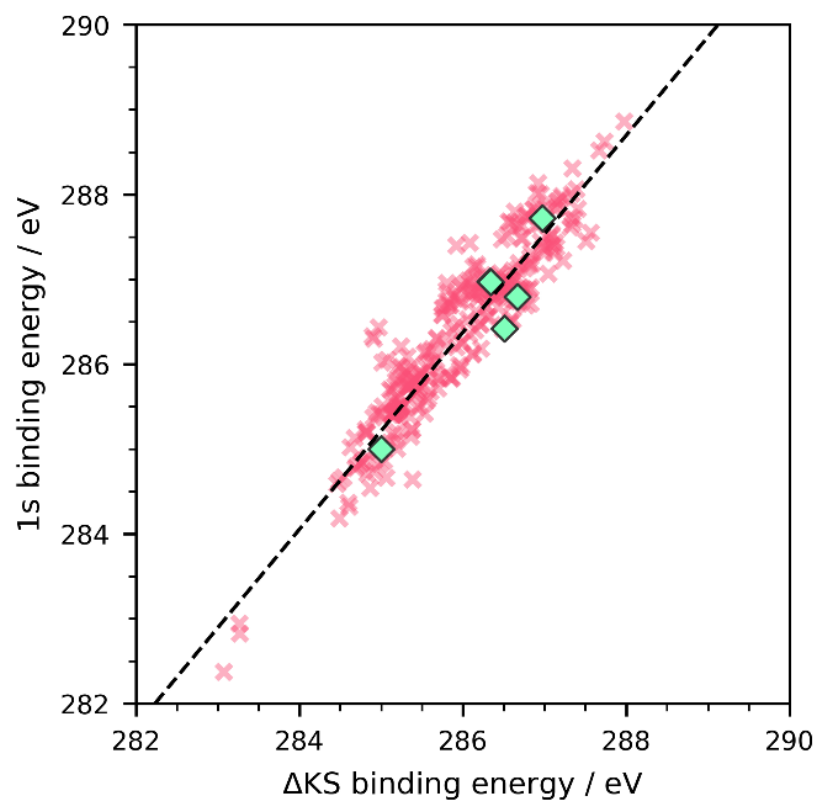


Figure 5. Comparison of calculated relative ΔKS with 1s binding energy values for C(1s) for forty ion pairs. The dashed line is the linear regression ($R^2 = 0.93$). Rhombs show values calculated for EMImBF₄.

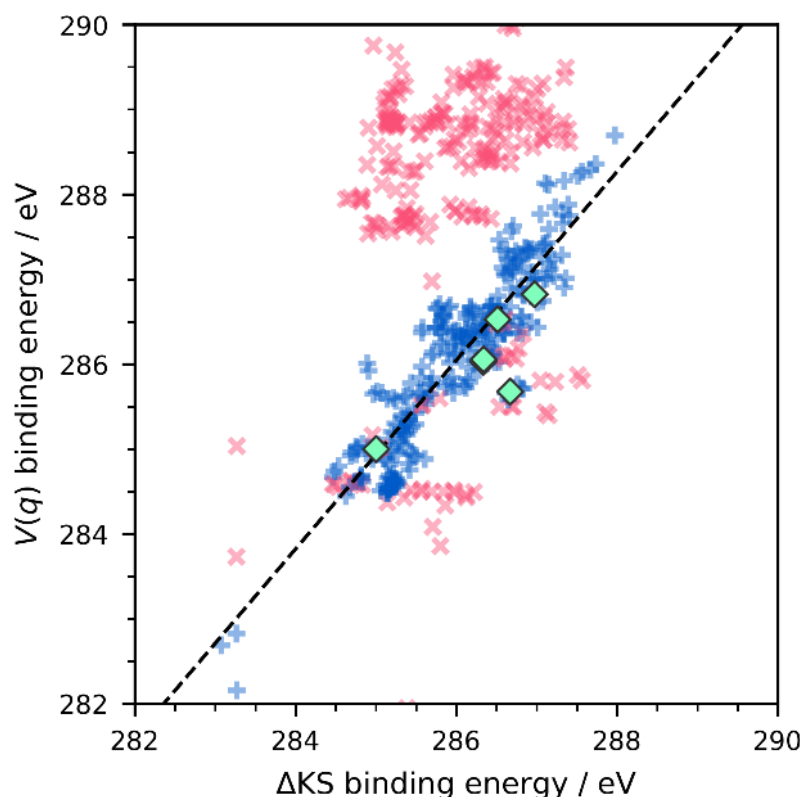


Figure 6. Comparison of calculated $V(q_i)$ (lighter red \times) and $V(q_i, q_j)$ (darker blue $+$) C(1s) binding energy values with the calculated relative Δ KS BE for forty ion pairs. The dashed line is the linear regression ($R^2 = 0.83$) for the $V(q_i, q_j)$ data. Rhombs show values calculated for EMImBF₄.

GRAPHICAL ABSTRACT

AUTHOR NAMES

Meeri Lembinen, Ergo Nõmmiste, Heigo Ers, Borja Docampo-Álvarez, Jaanus Kruusma, Enn Lust, and Vladislav B. Ivaništšev

TITLE

Calculation of core-level electron spectra of ionic liquids

TEXT

This study shows how the core-level binding energy values can be calculated and used to plot theoretical spectra using three density functional theory-based approaches: delta Kohn–Sham (Δ KS) calculations, 1s Kohn–Sham orbital energies, and atomic charges. A good agreement with the experimental X-ray photoelectron data has been established for the Δ KS results.

GRAPHICAL ABSTRACT FIGURE

